Changes in the Catalytic Properties of *p*-Hydroxybenzoate Hydroxylase Caused by the Mutation Asn300Asp†

Bruce A. Palfey,‡ Barrie Entsch,§ David P. Ballou,*,‡ and Vincent Massey‡

Department of Biological Chemistry, University of Michigan, Ann Arbor, Michigan 48109-0606, and Department of Biochemistry, Microbiology, and Nutrition, University of New England, Armidale, New South Wales 2351, Australia

Received July 15, 1993; Revised Manuscript Received November 3, 1993®

ABSTRACT: By site-directed mutagenesis, we have changed Asn 300 to Asp in *p*-hydroxybenzoate hydroxylase (PHBH; EC 1.14.13.2) from *Pseudomonas aeruginosa*. In the wild-type (WT) enzyme, residue 300 is in contact with the isoalloxazine ring of the active-site FAD; in the Asn300Asp mutant, this side chain has moved by about 5 Å, altering the protein structure [Lah, M. S., Palfey, B. A., Schreuder, H. A., & Ludwig, M. L. (1994) *Biochemistry* (following paper in this issue)]. The structural changes are responsible for profound catalytic and dynamic effects. The flavin of PHBH is reduced by NADPH in the first half of catalysis. The mutation has decreased this rate 330-fold, apparently by affecting the reactive orientation of the isoalloxazine and pyridine rings. Furthermore, the redox potential of the flavin is lower in the mutant enzyme than in WT by 20–40 mV. The reduced flavin of PHBH reacts with O_2 to form a flavin C(4a)-hydroperoxide, which is the species that transfers oxygen to the aromatic substrate. Previous studies indicated that the enzyme promotes the hydroxylation reaction in part by activating the substrate through lowering the phenolic pK_a. The Asn300Asp mutant does not lower the substrate pK_a. As a consequence of this, and also an enhanced stability of the flavin C(4a)-hydroperoxide, the hydroxylation is 50-fold slower in the mutant than in WT. However, despite the slow rate of the hydroxylation reaction, no H_2O_2 is formed by the competitive elimination reaction. The kinetic stability of the flavin C(4a)-hydroxide formed by the hydroxylation was also enhanced by the mutation. By studying the effects of the inhibitor azide on the oxidative sequence, we were able to conclude that the inhibitory site is readily accessible to solvent; azide binding at a second site slowly displaces the substrate from the reduced enzyme. The mutation has profoundly slowed the rates of ligand binding to the enzyme. Kinetic studies of binding indicated the presence of several enzyme conformations. Thus, the mutation of this one residue interferes with the orientation of pyridine nucleotide and flavin during reduction, stabilizes flavin C(4a) intermediates, prevents substrate ionization, and alters the rates and strengths of ligand binding.

Site-directed mutagenesis has become an important tool for probing the influence of protein structure on enzymatic catalysis. For most enzymes, however, individual catalytic steps are not directly observable, and the effects of mutations must be deduced by indirect steady-state kinetic methods. In contrast, the individual reaction steps of flavin-containing enzymes are easily observed by stopped-flow methods, making them ideal candidates for detailed studies on the involvement of protein residues in individual catalytic steps. *p*-Hydroxybenzoate hydroxylase (PHBH;[1] EC 1.14.13.2) catalyzes the hydroxylation of *p*-hydroxybenzoate (*p*-OHB) to form 3,4-dihydroxybenzoate (3,4-diOHB) as shown in eq 1. The active-site FAD serves as a spectral reporter group and has allowed the extensive study of the intermediates in the reductive and oxidative half-reactions (Howell *et al.*, 1972; Entsch *et al.*, 1976; Husain & Massey, 1979; Wessiak *et al.*, 1984; Entsch & Ballou, 1989; Schopfer *et al.*, 1991).

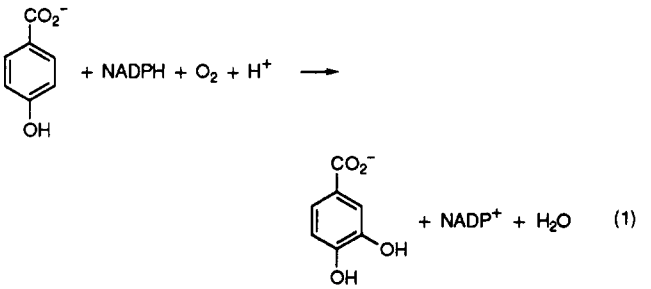

Studies from Drenth's group (Van der Laan, 1986; Schreuder *et al.*, 1988, 1989, 1992) have shown that PHBH binds the substrate, *p*-hydroxybenzoate, in a largely hydrophobic pocket next to N(5) of the flavin (Figure 1 and also figures from the accompanying paper). The carboxylate of the substrate is held by a salt bridge with an arginine and by hydrogen bonds to a serine and a tyrosine. The phenolic hydroxyl of the substrate hydrogen bonds to Tyr 201, which hydrogen bonds to Tyr 385, forming a hydrogen bond network.

This detailed structural information has come from X-ray studies of PHBH from *Pseudomonas fluorescens*. The gene from the enzyme from *Pseudomonas aeruginosa*, *pobA*, has been cloned and sequenced (Entsch *et al.*, 1988), and we are

† Supported by grants from the U.S. Public Health Service (GM 20877 to D.P.B., GM 11106 to V.M., GM 08270 to B.A.P.), the University of Michigan (Rackham Graduate School, Program to Support International Partnerships, D.P.B.; Rackham Graduate School Predoctoral Fellowship, B.A.P.), and the Australian Research Council (B.E.).

* To whom correspondence should be addressed at Department of Biological Chemistry, University of Michigan, Medical Science Building I, Box 0606, Ann Arbor, MI 48109-0606.

‡ University of Michigan.

§ University of New England.

® Abstract published in *Advance ACS Abstracts,* January 15, 1994.

[1] Abbreviations: PHBH, *p*-hydroxybenzoate hydroxylase; *p*-OHB, *p*-hydroxybenzoate; 2,4-diOHB, 2,4-dihydroxybenzoate; 3,4-diOHB, 3,4-dihydroxybenzoate; *p*-OHC, *p*-hydroxycinnamate; E_{ox}, enzyme with FAD in the oxidized form; EFlH$^-$, enzyme with FAD in the reduced form; EFlHOOH, enzyme with FAD in the C(4a)-hydroperoxide form; EFlHOH, enzyme with FAD in the C(4a)-hydroxide form; WT, wild-type PHBH; SDS–PAGE, sodium dodecyl sulfate–polyacrylamide gel electrophoresis; TN, turnover number.

0006-2960/94/0433-1545$04.50/0

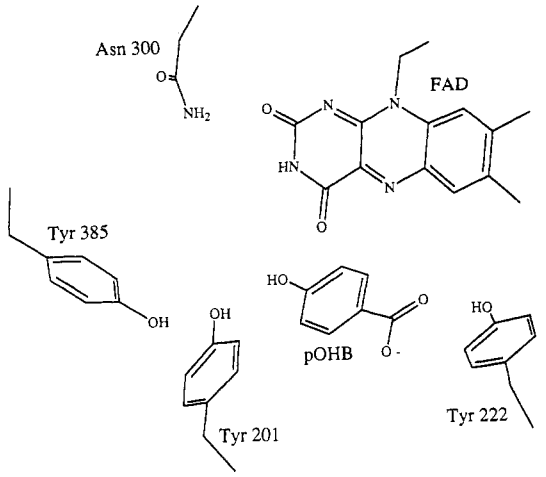

FIGURE 1: Active site of WT-PHBH as determined by Schreuder *et al.* (1989). The substrate of the reaction, *p*-OHB, is shown in its binding site near the flavin. The view is from the *re* side of the isoalloxazine ring, which is in the plane of the paper. The hydroxyl of *p*-OHB points toward the viewer.

using this gene for site-directed mutagenesis studies. X-ray diffraction studies on PHBH (mutants and WT) being conducted in the laboratory of M. Ludwig (Lah *et al.*, 1994) reveal that the structures of the enzyme from *P. fluorescens* and *P. aeruginosa*, which differ only in two surface residues, are the same. The ability to determine the structures of the PHBH mutants that we have constructed is allowing us to examine protein structure–function relationships in detail.

By substituting either Tyr 201 or Tyr 385 with Phe, we have shown that each of these tyrosines has multiple roles in catalysis (Entsch *et al.*, 1991b). The reduced flavin of PHBH, and of all other flavin monooxygenases studied, reacts with oxygen to form a C(4a)-flavin hydroperoxide (EFlHOOH) (Ballou, 1984). This flavin hydroperoxide can either productively hydroxylate the substrate or in an unproductive mode eliminate H_2O_2. Mutations of either tyrosine produce no structural perturbations (Lah *et al.*, 1994), but affect both the rates and the partitioning of the flavin hydroperoxide toward hydroxylation or H_2O_2 formation. Tyr 201, which forms a hydrogen bond to the hydroxyl of *p*-OHB, promotes effective ionization of the substrate to its phenolate form, thus activating it toward hydroxylation (Entsch *et al.*, 1991b). These results demonstrate that the protein influences the fate of the hydroperoxide by controlling the reactivity of the substrate.

In the current work, we sought to alter the reactivity of the flavin hydroperoxide by another protein mutation. It can be seen from the crystal structure that the isoalloxazine ring of FAD has several direct contacts with the protein (Schreuder *et al.*, 1989). Most of these involve hydrogen bonds from the protein backbone to the pyrimidine ring of the flavin. The only side chain interacting with the flavin is asparagine 300, which contacts the carbonyl oxygen at the 2-position of the flavin (see Figure 1). Asn 300 is at the start of helix H10, the longest α-helix in the protein and has been suggested to produce an electron-withdrawing effect on the FAD via its helix dipole, modulating the flavin reactivity (Schreuder *et al.*, 1990). Altering this residue might be expected to produce significant changes in both the oxidative and reductive half-reactions. This paper reports the dramatic functional changes caused by the mutation Asn300Asp. The structure of the mutant enzyme–*p*-OHB complex has been determined by X-ray diffraction and is reported in the accompanying paper (Lah et al., 1994).

MATERIALS AND METHODS

The Asn300Asp mutant was constructed from the *pobA* gene using the method of Kunkel *et al.* (1987) and expressed in *Escherichia coli* as described previously (Entsch *et al.*, 1991b). The mutant sequence was confirmed using the dideoxynucleotide procedure previously described (Entsch *et al.*, 1991b).

PHBH (mutant and WT) was purified either by published methods (Entsch, 1990; Müller *et al.*, 1979; Entsch *et al.*, 1976) or by a new procedure, developed because the Blue Sepharose column of the published procedure failed to bind the mutant PHBH. In the new procedure, the initial steps of the standard purification (Entsch, 1990) were followed. Then, the 43% $(NH_4)_2SO_4$ supernatant was concentrated by precipitating the protein with $(NH_4)_2SO_4$ (to 70% saturation) and dissolving the precipitate in 10 mM Tris–maleate and 0.3 mM EDTA, pH 7.0 (affinity buffer). The protein solution was dialyzed overnight at 4 °C against affinity buffer and then heat-treated (40 °C) for 15 min. Precipitated protein was removed by centrifugation (20 000 rpm for 30 min), and the yellow supernatant was applied to a 100–150-mL column of Procion Red-A (Matragel Red-A, Amicon) equilibrated in affinity buffer. It was found that at low ionic strength this column binds PHBH by displacing FAD from the enzyme. The column was washed with 300 mL of affinity buffer to remove free FAD and contaminating proteins and then was washed with 300 mL of 50 mM KP_i, 1 mM EDTA, and 0.5 mM *p*-OHB, pH 7.0. The enzyme was eluted by washing with the same buffer +25 μM FAD. The yellow fractions were pooled, concentrated using an Amicon PM-30 membrane, precipitated with $(NH_4)_2SO_4$, and pelleted by centrifugation. The enzyme was dissolved in 50 mM KP_i and 1 mM EDTA, pH 7.0, and free FAD was removed by gel filtration. PHBH was stored as an $(NH_4)_2SO_4$ precipitate at 4 °C. By this method we obtained PHBH (which was routinely used for experiments) that had an A_{280}/A_{450} of about 10–12, with no contamination from chromophores in the visible region. Further purification by mono-Q FPLC yielded enzyme that was homogeneous by SDS–PAGE and unchanged in its kinetic properties. The Asn300Asp mutant was obtained in about half the yield of the WT enzyme. Unlike the WT enzyme, significant amounts of the mutant protein denatured during the heat treatment, accounting for the poorer yield.

Stopped-flow experiments were conducted using an instrument constructed here and described previously (Entsch *et al.*, 1991b), a Kinetic Instruments, Inc. stopped-flow spectrofluorimeter for monitoring fluorescence changes or a Hi-Tech Scientific SF-61 stopped-flow instrument for measuring absorbance and fluorescence changes.

All other reagents and analytical methods were as described (Entsch *et al.*, 1991b).

RESULTS

Enzyme Purification. We have developed a novel method for purifying PHBH, based on the observation that the dye of Red-A Matragel displaces FAD from PHBH upon binding the enzyme (Materials and Methods). Dyes commonly used for affinity chromatography are thought to act as nucleotide analogs. The displacement of FAD from PHBH is in keeping with the previously reported behavior of pyridine nucleotide analogs that displace FAD from the active site (van der Laan *et al.*, 1989). It is interesting to note that the displacement of FAD from phenol hydroxylase by Cibacron Blue has been reported (Sejlitz & Neujahr, 1987), although no use of this

Table 1: General Properties of Asn300Asp Compared to WT

	K_d (μM)[b]	
max TN, pH 6.5, 4 °C	WT[a] (5.7 s^{-1})	Asn300Asp (0.06 s^{-1})
p-OHB	9.5	7.8
2,4-diOHB	22	104
3,4-diOHB	230	69
p-OHC	100	1000
NADPH[c]	210	990
relative fluorescence[d,e]	0.99	0.23
+*p*-OHB	0.26	0.10
E_{m7}, free enzyme[d] (mV)	−163	−180
E_{m7}, +*p*-OHB (mV)	−165	−205

[a] Values from Entsch *et al.* (1991b). [b] Dissociation constants were determined at 4 ° in 50 mM KP_i and 1 mM EDTA, pH 6.5. [c] Dissociation constant from the enzyme–*p*-OHB complex. [d] Determined at 25 °C in 0.1 M KP_i, pH 7.0. [e] Fluorescence relative to FAD.

phenomenon was made for purification. This riases the intriguing possibility that the family of flavoprotein hydroxylases might be purified by displacing the flavin with a suitable dye column and eluting with FAD.

Physical Properties. The mutation changed the spectral properties of the enzyme-bound flavin. The visible peak was shifted from 450 to 454 nm at pH 6.5 and pH 7.0. A comparison of the spectrum of Asn300Asp in 0.1 M NaP_i, pH 7.0, 25 °C, to the spectrum of the FAD liberated from this sample by the addition of SDS to 0.1% saturation allowed the calculation of ϵ_{450} of 9.80 mM^{-1} cm^{-1}, compared to 10.3 mM^{-1} cm^{-1} found for WT enzyme (Entsch *et al.*, 1991b). In contrast to the WT enzyme, which has a fluorescence intensity similar to free FAD (Entsch *et al.*, 1991b), the fluorescence of the oxidized enzyme was decreased to 23% of free FAD (Table 1).

The two-electron redox potential of the flavin in the mutant was measured (Figure 2, Table 1) at pH 7, 25 °C. The substrate-free mutant enzyme had a potential 20 mV lower than that of WT enzyme, and the potential of the Asn300Asp·*p*-OHB complex was lower by 40 mV than that of WT enzyme; the potential of the WT enzyme did not change with *p*-OHB binding. These observations are consistent with a new negative charge near the flavin, making the reduction of the flavin more difficult.

Ligand Ionization. Ionization of the substrate phenol has been identified as a mechanism of substrate activation. This effect was emphasized in studies of the Tyr201Phe and Tyr385Phe mutants (Entsch *et al.*, 1991b), where the ionization to the enzyme-bound phenolate was observed by difference spectroscopy. Similar experiments were performed with Asn300Asp. No ionization of mutant-bound *p*-OHB was observed, up to pH 8.5. The lack of stabilization of the phenolate form of *p*-OHB is interpreted to have important catalytic consequences (see Discussion). The ionization of another substrate, 2,4-dihydroxybenzoate (2,4-diOHB), was also investigated. Neither WT enzyme nor Asn300Asp showed signs of lowering the pK_a of 2,4-diOHB, a substrate that is hydroxylated slower than *p*-OHB by WT enzyme.

p-Hydroxycinnamate (*p*-OHC) is an inhibitor with convenient spectral properties. The pK_a of *p*-OHC decreases by about 2 units upon binding to WT enzyme and to Tyr385Phe, but not when bound to Tyr201Phe (Entsch *et al.*, 1991b). The ionization of *p*-OHC bound to Asn300Asp was clearly observed, with a pK_a of 7.2, compared to 6.9 when bound to WT enzyme and 9.3 when free in solution. The K_d for this ligand with Asn300Asp was 1 mM, about 10-fold higher than for WT enzyme. Thus, in contrast to the behavior of the WT enzyme and the two previously studied mutants, *p*-OHB and

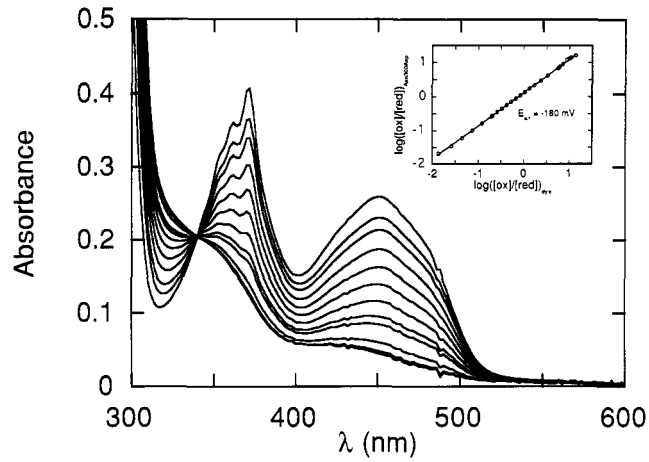

FIGURE 2: Determination of the redox potential of Asn300Asp. Anaerobic enzyme (20 μM) and 1-hydroxyphenazine (25 μM) were catalytically reduced by xanthine (200 μM), xanthine oxidase, and benzyl viologen (2 μM) in 0.1 M NaP_i, pH 7.0, at 25 °C, and the reactions were followed spectrally (Massey, 1991). Inset: The reduction of 1-hydroxyphenazine was monitored by the decrease in absorbance at 370 nm, and the reduction of Asn300Asp was monitored by the decrease in absorbance at 480 nm, allowing the ratios of oxidized and reduced species to be calculated. A potential of −172 mV for the 1-OH phenazine couple was used to determine the potential of the enzyme.

p-OHC had distinguishable effects upon binding to Asn-300Asp.

Catalysis. Catalysis was studied in 50 mM KP_i and 10 mM EDTA, pH 6.5, 3 °C, conditions that are well suited to the resolution of reaction intermediates in the WT enzyme (Entsch *et al.*, 1976). Wild-type enzyme catalyzes the reaction shown in eq 1 with a maximum turnover number under these conditions of 5.7 s^{-1} (Entsch *et al.*, 1991b). The mutant enzyme catalyzed the reaction with a maximum turnover number of 0.060 s^{-1} as measured by enzyme-monitored turnover (Gibson *et al.*, 1964). There was even more than a 100-fold difference at pH 8.0, 25 °C, the conditions for optimum activity of WT enzyme. Nevertheless, product analysis by HPLC showed that *p*-OHB was hydroxylated to 3,4-diOHB with a stoichiometric consumption of NADPH. There was no indication of any other hydroxylation products being formed (<1 μM) after a 17-h incubation (>10 000 turnovers).

Reductive Half-Reaction. The reduction of the mutant enzyme was studied in a stopped-flow spectrophotometer by mixing the anaerobic enzyme–*p*-OHB complex with anaerobic solutions of NADPH and *p*-OHB (15 μM Asn300Asp, 500 μM *p*-OHB, after mixing). The reactions were observed at 450 nm and fitted to biphasic exponential curves. The decrease in absorbance was dominated by the faster phase (approximately 85% of the total change). The reaction was extremely slow compared to WT enzyme. The observed rate constant for the first phase showed a hyperbolic dependence on NADPH concentration, allowing us to calculate a K_d of 0.99 mM for NADPH from the NADPH·Asn300Asp·*p*-OHB complex and a limiting reduction rate of the enzyme flavin of 0.15 s^{-1}, 330-fold lower than for WT enzyme. Flavin–NADP(H) charge transfer intermediates, detectable with WT enzyme at 720 nm (Howell *et al.*, 1972), were not observed.

The second, slower rate observed at 450 nm (3.8×10^{-3} s^{-1}) was independent of NADPH concentration. The rate and extent of this phase varied with the wavelength of observation. The probable nature of this phase became apparent at wavelengths between 520 and 720 nm, where a broad, low

Table 2: Oxidative Reaction Rate Constants[a]

EFlH⁻·*p*-OHB + O_2	k_1	EFlHOOH·*p* OHB	k_2	EFlHOH·3,4-diOHB	k_3	E_{ox}·*p*-OHB
WT	2.8×10^5 M^{-1} s^{-1}		47 s^{-1}		14 s^{-1}	
WT + N_3^-	2.7×10^5 M^{-1} s^{-1}		6.5 s^{-1}		1.5 s^{-1}	
Asn300Asp	3.9×10^5 M^{-1} s^{-1}		1.1 s^{-1}		0.12 s^{-1}	
Asn300Asp + N_3^-	2.8×10^5 M^{-1} s^{-1}		0.8 s^{-1}		0.09 s^{-1}	

EFlH⁻ + O_2	k_1	EFlHOOH	k_2	E_{ox}
WT	2.6×10^4 M^{-1} s^{-1}		fast[b]	
WT + N_3^-	2.6×10^4 M^{-1} s^{-1}		3.4 s^{-1}	
Asn300Asp	3.2×10^4 M^{-1} s^{-1}		fast[b]	
Asn300Asp + N_3^-	2.8×10^4 M^{-1} s^{-1}		2.7 s^{-1}	

[a] Values for WT are from Entsch *et al.* (1991b, 1976). [b] EFlHOOH cannot be detected; its rate constant for decomposition is much greater than for formation.

absorbance formed during reduction. This absorbance is characteristic of the neutral flavin semiquinone (Massey & Palmer, 1966), which probably formed photochemically. Whatever the mechanism of formation of this species, it is clear that 10–15% of the enzyme was trapped in the semiquinone form during the reduction, and this subsequently reacted in the very slow phase, which was too slow to contribute to the measured turnover rate.

In the absence of substrate, the mutant and WT enzyme were reduced by NADPH at similar rates. For instance, with 2.2 mM NADPH, a pseudo-first-order rate constant of 0.058 min^{-1} was observed for the mutant, while one of 0.024 min^{-1} was observed for the WT enzyme (Entsch *et al.*, 1991b). The discrepancy between this slow rate and the abnormally high rate reported previously for this mutant (Entsch *et al.*, 1991a) was due to substrate contamination of the enzyme used in the earlier study. It has been found that substrate dissociates slowly from the oxidized flavin form of the mutant enzyme and is not removed quantitatively by the standard gel filtration columns, which were routinely used to prepare the WT enzyme for study (see below).

Oxidative Half-Reaction. The reaction of the reduced Asn300Asp·*p*-OHB complex with oxygen was followed by stopped-flow spectrophotometry over the wavelength range 320–520 nm. These data were used to calculate absorbance spectra of the intermediates. The results are summarized in Table 2 and Figure 3. Three consecutive reactions were observed, as with WT enzyme. The first reaction was the fast second-order formation of the flavin–C(4a)-hydroperoxide (Figure 3). The mutant reacted with oxygen with a rate constant of 3.9×10^5 M^{-1} s^{-1}, compared to 2.5×10^5 M^{-1} s^{-1} for WT enzyme. The terminal oxygen of the hydroperoxide is then transferred to the substrate to form 3,4-diOHB. In WT enzyme, a blue shift occurs in the spectrum of the flavin-C(4a) derivative during this reaction. With the mutant, no blue shift was observed during this reaction—the spectra of EFlHOOH and EFlHOH were essentially identical. With minimal changes in absorbance in this reaction (Figure 4), the rate of the hydroxylation reaction was difficult to determine accurately, but was estimated to be 1 s^{-1} by simulating the reaction traces with a computer program for consecutive reactions (developed by Dr. Christopher Batie in this laboratory). The third reaction in the oxidative sequence is the release of the product and the elimination of water from the C(4a)-hydroxyflavin to form oxidized enzyme. This final reaction (k = 0.125 s^{-1}) was more than 100-fold slower than with the WT enzyme and was easily measured at most wavelengths.

Fluorescence changes observed with this reaction confirmed the above results. We observed the rapid formation of a weakly fluorescent species from the reaction of the nonfluorescent

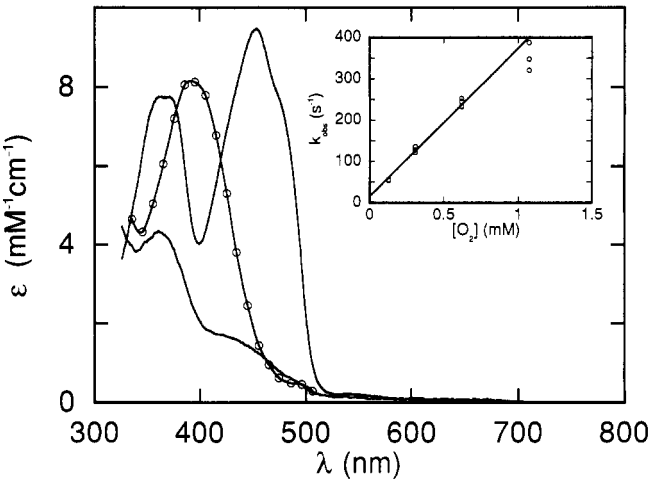

FIGURE 3: Spectra of the reduced, EFlHOOH, and oxidized forms of Asn300Asp. The enzyme–*p*-OHB complex was made anaerobic, reduced with dithionite, and reacted in a stopped-flow spectrophotometer by mixing with oxygen-equilibrated buffer. The lower curve is the spectrum of the reduced enzyme. Upon mixing with O_2, the flavin hydroperoxide (open circles) is formed. The spectrum of this species was determined by observing the reaction at a series of wavelengths. Unlike the WT enzyme, the spectrum of EFlHOH (formed after EFlHOOH hydroxylates the substrate) does not differ significantly from the spectrum of EFlHOOH. The reactions were in 50 mM KP_i and 10 mM EDTA, pH 6.5, at 4 °C. The final concentrations were 15 μM enzyme, 500 μM *p*-OHB, and 610 μM O_2. Inset: The dependence of the observed rate constant for the formation of EFlHOOH on oxygen concentration.

EFlH⁻ and O_2 at the same rate observed for the formation of EFlHOOH by absorbance (Figure 4). This was followed by a large increase in fluorescence at a rate of 1.1 s^{-1}, during which no significant change in absorbance occurred at any wavelength. This highly fluorescent species decayed at a rate of 0.14 s^{-1}. The rates of formation and decay of this fluorescent species agree well with the simulated hydroxylation rate and the observed elimination of water from EFlHOH from absorbance stopped-flow experiments. Thus, although EFlHOOH and EFlHOH of the mutant had the same absorbance spectrum, the hydroxyflavin had a significantly higher fluorescence quantum yield than the hydroperoxyflavin, allowing the direct observation of the hydroxylation reaction.

After the substantial decrease in fluorescence corresponding to the conversion of EFlHOH to E_{OX}, additional very slow changes in fluorescence were observed. These reactions involved only a small proportion of the enzyme and were photochemical in nature. When the excitation light intensity was increased by using larger slit widths, a larger proportion of enzyme formed this slowly decaying fluorescent species. We believe that this species was a dead-end complex of EFlHOH and *p*-OHB.

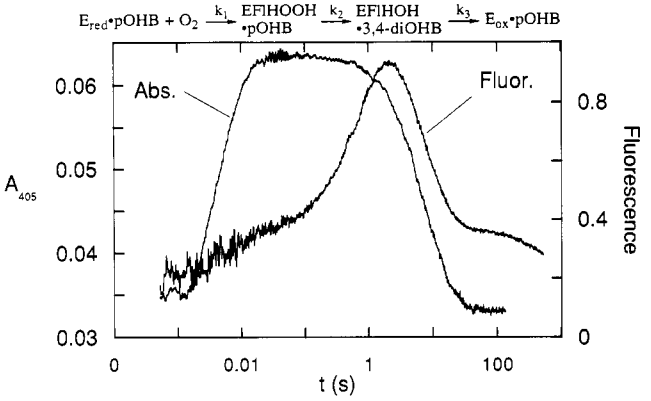

FIGURE 4: Kinetic traces of the oxidative half-reaction of reduced Asn300Asp observed by absorbance and fluorescence. The reduced enzyme–*p*-OHB complex was reacted with 0.6 mM oxygen under the conditions given for Figure 3. The reaction was followed either by absorbance (405 nm) or fluorescence (λ_{ex} = 404 nm, 4-nm band pass, λ_{em} > 510 nm). Note the logarithmic time scale, which allows all phases of the reaction to be displayed on the same graph. The mutant enzyme hydroxylates *p*-OHB to form EFlHOH·3,4-diOHB (around 1 s). The absorbance change that is seen for this reaction with WT enzyme is absent in the mutant enzyme. However, this reaction produces a significant increase in fluorescence, allowing the direct observation of the hydroxylation reaction. The slowly decaying fluorescence after 100 s is ascribed to EFlHOH complexed with *p*-OHB, which is formed photochemically from EFlHOH·3,4-diOHB. The values for k_1, k_2, and k_3 are given in Table 2.

Azide Effects. The inhibitory effects of monovalent anions such as azide on PHBH have been known for some time (Steennis *et al.*, 1973). In the WT enzyme, azide inhibits steps in both half-reactions and has been employed advantageously to slow some of the steps of the oxidative half-reaction. Qualitatively, the effects of the Asn300Asp mutation on the oxidative half-reaction are similar to the effects that azide has on the WT enzyme. Since the origin of the azide effects is still not known, it was of further interest to define the similarities and differences between Asn300Asp and WT enzyme complexes with N_3^-.

We investigated the effect azide has on the hydroxylation of *p*-OHB by the mutant by mixing the reduced mutant–*p*-OHB complex with buffer containing oxygen and sodium azide (0.1 M, final) in a stopped-flow spectrophotometer. As with WT PHBH, azide did not affect the rate at which reduced Asn300Asp reacted with O_2 to form EFlHOOH. However, with WT enzyme, 0.1 M azide slowed the conversion of EFlHOOH to EFlHOH by a factor of 6.6 ($\Delta\Delta G^{\ddagger}$ = 1.0 kcal mol^{-1}) and slowed the conversion of EFlHOH to the oxidized enzyme by a factor of 6.9 ($\Delta\Delta G^{\ddagger}$ = 1.1 kcal mol^{-1}). With the mutant, the effects of azide were much smaller; azide slowed the reactions only by factors of about 1.2 ($\Delta\Delta G^{\ddagger}$ = 0.10 kcal mol^{-1}) and 1.4 ($\Delta\Delta G^{\ddagger}$ = 0.19 kcal mol^{-1}), respectively (Table 2). Thus, azide bound to the mutant, but exerted only a small additional inhibitory effect beyond that provided by the mutation.

In the absence of substrate, both the WT and mutant enzymes reacted similarly with O_2. The reduced WT enzyme reacts with O_2 about 10-fold slower than in the presence of substrate; no oxygenated flavin intermediates are observable. Free Asn300Asp also reacted with O_2 at the same rate (k = 3 × 10^4 M^{-1} s^{-1}) to form oxidized enzyme without any detectable intermediates. Including 0.1 M azide in the reaction mixtures alters the reaction of the free mutant and WT enzymes (Entsch *et al.*, 1976). A total of 60% EFlHOOH is observed, which then eliminates H_2O_2 at a rate of about 3 s^{-1} for both enzymes. Thus, the effects of azide on WT enzyme are only mimicked in the mutant when *p*-OHB (or other substrates; unpublished results) is bound to the enzyme.

We detected two distinct azide binding sites. Azide binds quickly to the first site; binding at this site is responsible for the inhibitory effects. Binding to the second site was slow and caused the dissociation of *p*-OHB from the enzyme. This second binding was observed when 0.1 M azide was included with both the reduced mutant–*p*-OHB complex and in the oxygen buffer for stopped-flow experiments. In contrast to WT enzyme, where there was no difference whether azide was included with the enzyme or introduced only in the oxygen syringe (Entsch *et al.*, 1976), preincubating the reduced mutant enzyme with azide and substrate produced complex absorbance traces with five phases at some wavelengths. Two phases showed a linear dependence on oxygen concentration. The larger second-order rate constant (2 × 10^5 M^{-1} s^{-1}) was the same as the second-order rate constant observed when azide-free Asn300Asp·*p*-OHB was reacted with oxygenated buffer containing azide. The smaller second-order rate constant (3 × 10^4 M^{-1} s^{-1}) agreed with the second-order rate constant obtained by reacting ligand-free Asn300Asp with oxygenated buffer containing azide. Thus, it appears that two parallel reaction paths, one of free enzyme reacting with oxygen and the other of enzyme–substrate complex reacting with oxygen, were occurring. Analysis of the absorbance traces at various wavelengths gave the same rate constants previously measured independently for both these reaction paths. Therefore, an extended incubation of Asn300Asp with azide does not alter the rate constants on the hydroxylation pathway. The effect of azide on the reactions in the hydroxylation pathway is thus due to a site (or sites) that is (are) rapidly accessible, not to binding to any slow, inhibitory anion binding site.

The fact that upon incubation of the reduced enzyme with substrate and azide a substantial amount of enzyme did not have *p*-OHB bound reveals an unexpected result—azide competes with *p*-OHB binding to the mutant. This was not seen when azide-free Asn300Asp·*p*-OHB is mixed with azide-containing oxygen buffer, where all the enzyme hydroxylated the substrate. Thus, azide displaces *p*-OHB slowly, whereas stabilization of the hydroperoxide by azide is due to its binding at a rapid binding site rather than to the substrate binding site.

Ligand Binding. The binding constants for a variety of ligands were determined by titrating the enzyme with a concentrated solution of the ligand and recording the spectral changes caused by binding (see Figure 5 as an example). The resulting flavin difference spectra were quite distinct from those obtained for WT enzyme. The mutation caused a variety of effects on ligand binding strength. The natural substrate, *p*-OHB, binds to Asn300Asp with essentially the same affinity as WT enzyme (Table 1). An alternate substrate, 2,4-diOHB, binds more weakly to the mutant enzyme with a K_d about 3-fold higher than WT enzyme. The product of *p*-OHB hydroxylation, 3,4-diOHB, binds more tightly to Asn300Asp with a K_d about three times lower than WT enzyme.

Anomalous behavior by the mutant enzyme in the substrate-free reduction reaction led us to investigate the kinetics of ligand binding. It was found that *p*-OHB and 3,4-diOHB bind to the oxidized mutant enzyme at rates measurable by stopped-flow methods. This is in contrast to the oxidized WT enzyme, which binds these ligands within the dead time (≤3 ms) of the instruments (Entsch *et al.*, 1976). Ligand binding was measured by observing the small absorbance or fluorescence changes in the enzyme-bound FAD.

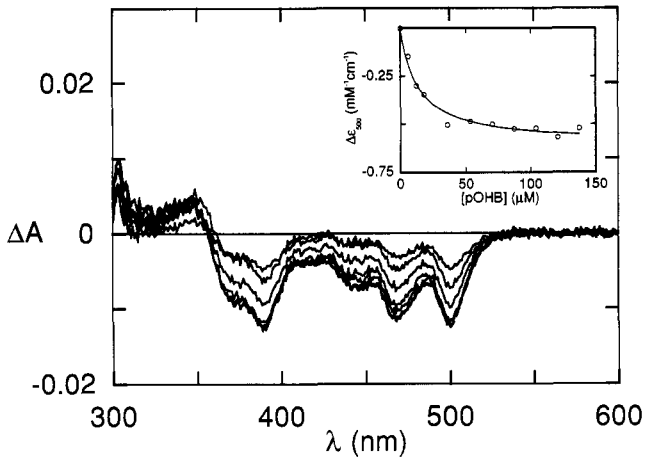

FIGURE 5: Dissociation constant of the enzyme–*p*-OHB complex. The dissociation constant of *p*-OHB from the mutant enzyme was determined by titrating Asn300Asp (20 μM) in 50 mM KP_i and 1 mM EDTA, pH 6.5, 4 °C, with *p*-OHB by adding small aliquots of a concentrated *p*-OHB stock solution. Absorbance spectra were recorded, and difference spectra were calculated by subtracting the spectrum of ligand-free enzyme from all spectra. Inset: The dissociation constant was determined from the change in extinction coefficient at a suitable wavelenth (500 nm).

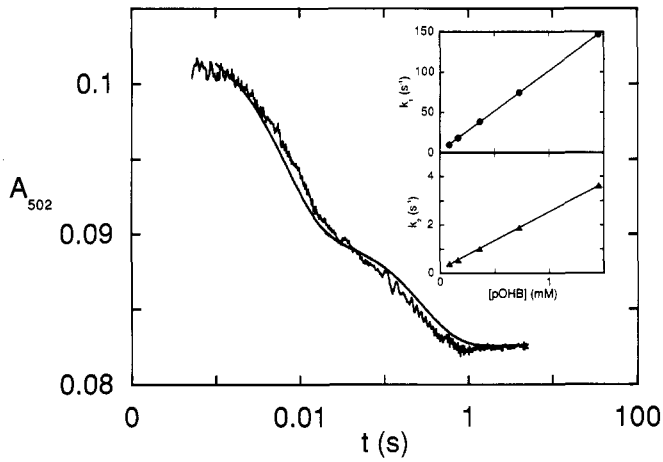

FIGURE 6: Binding kinetics of *p*-OHB. The kinetics of *p*-OHB binding to 10 μM Asn300Asp were determined in 50 mM KP_i and 1 mM EDTA, pH 6.5, at 4 °C, by observing the changes in absorbance at 502 nm after mixing the free enzyme with various concentrations of *p*-OHB. The data obtained for [*p*-OHB] = 1.45 mM are plotted with an absorbance trace simulated by the numerical solution of the rate equations. Note the logarithmic time scale. Constants used for the simulation (see Scheme 1): $k_{+1} = 9.9 \times 10^4$ M^{-1} s^{-1}, $k_{-1} = 2.0$ s^{-1}, $k_{+2} = 2.4 \times 10^3$ M^{-1} s^{-1}, $k_{-2} = 0.02$ s^{-1}, $k_{+iso} = 0.29$ s^{-1}, $k_{-iso} = 0.1$ s^{-1}, $\epsilon(E_1) = 4400$ M^{-1} cm^{-1}, $\epsilon(C_1) = 2280$ M^{-1} cm^{-1}, $\epsilon(E_2) = 4120$ M^{-1} cm^{-1}, and $\epsilon(C_2) = 3750$ M^{-1} cm^{-1}. Inset: The first two observed rate constants at different *p*-OHB concentrations, determined by fitting the experimental absorbance traces to three exponentials, are compared to rate constants determined by fitting three exponentials to absorbance traces simulated using the listed rate constants and extinction coefficients at several concentrations of *p*-OHB. The experimentally determined rates for the first phase are marked by ●, and the experimentally determined rates for the second phase are marked by ▲. The lines represent the rates derived from the fits to the simulations.

When observed by absorbance, the binding of *p*-OHB to the mutant enzyme was triphasic. These phases involved small absorbance changes and were difficult to determine precisely. The first two observed rates for *p*-OHB binding varied linearly with concentration (Figure 6), and the last observed rate showed no obvious concentration dependence. Many models might explain this behavior. A simple model that is consistent with the binding behavior of *p*-OHB is shown in Scheme 1.

Scheme 1: Binding of *p*-OHB to Asn300Asp[a]

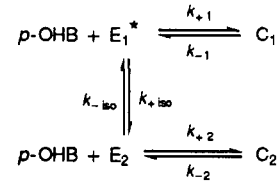

[a] The species with fluorescence that is quenched by binding ligand is marked by an asterisk (*).

Scheme 2: Binding of 3,4-diOHB to Asn300Asp[a]

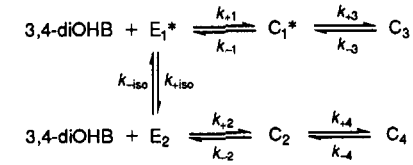

[a] The species with fluorescence that are quenched by binding ligand are marked by an asterisk (*).

The free enzyme exists as a slowly equilibrating mixture of two conformations. Each of these conformations binds *p*-OHB in a single step. Thus, the two rates that vary linearly with *p*-OHB concentration are due to the two independent bimolecular reactions. Binding of *p*-OHB to the two enzyme forms with different affinities perturbs the equilibrium between these two conformations; the third phase represents the slow re-equilibration between the two enzyme forms. From this model, the apparent K_d measured by spectral titrations is a function of the equilibrium constants of each step:

$$K_{d,app} = \frac{1 + K_{iso}}{1/K_1 + K_{iso}/K_2}$$

where K_1 and K_2 are the dissociation constants of *p*-OHB from C_1 and C_2, the two conformations of the mutant–*p*-OHB complex, and K_{iso} is the equilibrium constant between the two conformations of free enzyme, E_1 and E_2 ($K_{iso} = E_2/E_1$). Using the experimentally observed value for the apparent K_d of 8 μM as a constraint, we found a set of rate constants (Figure 6) that could be used to simulate the *p*-OHB binding kinetics with the program KinSim (Barshop *et al.*, 1983).

When the mutant enzyme was mixed with the product 3,4-diOHB in the absorbance stopped-flow spectrophotometer, triphasic kinetics were again observed. In contrast to the comparatively simple situation with *p*-OHB described above, the first two observed rates saturated hyperbolically with 3,4-diOHB concentration, suggesting that there are enzyme–3,4-diOHB complexes formed prior to the processes observed. The last observed rate showed no concentration dependence. Thus, the model in Scheme 1 must be modified to account for extra steps (Scheme 2), where the initial enzyme–3,4-diOHB complexes are in rapid equilibrium, followed by slower isomerization steps. From this model

$$K_{d,app} = \frac{1 + K_{iso}}{1/K_1 + 1/K_1K_3 + K_{iso}/K_2 + K_{iso}/K_2K_4}$$

where K_1 and K_2 are the dissociation constants of 3,4-diOHB from complexes C_1 and C_2, K_3 and K_4 are equilibrium constants for the isomerization of the mutant–3,4-diOHB complexes in the direction of dissociation ($K_3 = C_1/C_3$ and $K_4 = C_2/C_4$), and K_{iso} is the previously defined isomerization equilibrium constant for free enzyme. From the experimentally determined maximum and minimum rate constants for the first two phases of 3,4-diOHB binding, values for K_3 and K_4 were estimated by $K_3 = k_{+3}/k_{-3}$ and $K_4 = k_{+4}/k_{-4}$, where the values for k_{+n}

were taken as the rate constants at saturating 3,4-diOHB (198 and 8.9 s^{-1}), and the values for k_{-n} were taken as the rate constants extrapolated to zero concentration (4.6 and 0.21 s^{-1}) (Strickland *et al.*, 1975), giving K_3 = 0.023 and K_4 = 0.024. Values for K_1 and K_2 of 2.3 and 2.9 mM were obtained from the half-saturation points of plots of the observed rate constants as a function of 3,4-diOHB concentration. Using these values and the value of K_{iso} = 2.9 used for *p*-OHB binding (it should be independent of the identity of the ligand), a $K_{d,app}$ = 62 μM is calculated, in good agreement with the value of 70 μM found by spectral titrations.

Free Asn300Asp is only 23% as fluorescent as WT enzyme. We observed the quenching of the low Asn300Asp flavin fluorescence in the stopped-flow instrument when *p*-OHB or 3,4-diOHB was mixed with the mutant enzyme. For both ligands, only one phase was observed. The observed rate constants agree well with the fastest phases seen by absorbance. Thus, the quenching of fluorescence corresponds to the formation of C_1 from E_1 for *p*-OHB (Scheme 1) or the formation of C_3 from E_1 and C_1 for 3,4-diOHB (Scheme 2). Interestingly, the value of K_{iso} of 2.9 predicts that 26% of the free enzyme should be found in the E_1 form, nearly identical to the 23% fluorescence remaining after the mutation; perhaps, then, the free mutant enzyme is a mixture of enzyme which is about as fluorescent as WT enzyme (23% E_1) and a non-fluorescent form (77% E_2).

While the models presented for ligand binding seem to be consistent with our data, we must emphasize that our results are not conclusive, nor is it possible at this time to exclude other models for ligand binding. It is clear, however, that the mutation has drastically slowed the rates at which PHBH binds ligands, and the binding process is not simple.

DISCUSSION

The change of a nitrogen to an oxygen atom in the mutant, Asn300Asp, has profound effects on the enzyme. The mutant, like the WT enzyme, catalyzes the complex, multi-step hydroxylation of the substrate without the wasteful production of H_2O_2, but at a rate about 100-fold slower. Chemical and dynamic processes in catalysis are much slower than in the WT enzyme and account for the diminished turnover rate.

Ligand Binding. The bound substrate is not directly accessible to the solvent. The crystal structures show that protein movement is required for ligands to gain access to the active site in both WT and mutant enzymes (Schreuder *et al.*, 1989; Lah *et al.*, 1994). The slow, complex ligand binding by Asn300Asp indicates that the mutation has altered the dynamic behavior of the protein, since in WT enzyme, the equivalent processes are too fast to observe by stopped-flow methods. It is unclear how changing Asn 300 to Asp has altered this process, since the proposed route for ligand entry is somewhat removed from the mutation site (>12 Å). Crystal structures show that the mutated residue 300 has moved from its position in WT enzyme of contact with the C2 carbonyl of FAD to form a new hydrogen bond with Lys 297 (Lah *et al.*, 1994). This Lys also participates in a hydrogen bond to the peptidyl carbonyl (in both WT and the mutant enzymes) of Tyr 385. Perhaps the new Asp-Lys hydrogen bond contributes to the change in active-site dynamics. It should be noted that upon reduction the rate of binding of *p*-OHB to the WT enzyme drops dramatically, although the K_d is unaltered (Entsch *et al.*, 1976). Thus, this mutation seems to be mimicking a natural property of the WT enzyme.

Reductive Half-Reaction. The reduced form of the enzyme is destabilized by the mutation by 1.8 kcal mol^{-1} at pH 7.0, 25 °C, calculated from the reduction potential in the presence of substrate (Table 1). The change in reduction potential may be due to the electrostatic interaction of the reduced flavin anion with the negative charge of Asp 300. The crystal structure shows a slightly altered orientation of helix H10 which might also contribute to this effect (Lah *et al.*, 1994).

The binding of *p*-OHB to the oxidized WT enzyme stimulates the reduction of the enzyme-bound FAD by NADPH by a factor of about 10^4–10^5 (Howell *et al.*, 1972; Husain & Massey, 1979; Shoun *et al.*, 1979). The mutant does not retain this degree of stimulation, largely because of a decrease in the reduction rate of the Asn300Asp·*p*-OHB complex. In the presence of saturating *p*-OHB and NADPH, the rate of hydride transfer from NADPH to FAD in the mutant is about 330-fold slower than in WT enzyme (4 °C, pH 6.5), corresponding to a $\Delta\Delta G^{\ddagger}$ = 3.2 kcal mol^{-1}. The origin of this rate decrease may be rationalized by a Marcus-type analysis (Lowry & Richardson, 1987; Sühnel & Schowen, 1991). Marcus theory expresses the activation energy ($\Delta G^{\ddagger}$) of a reaction in terms of an "intrinsic" barrier energy (λ) that is modulated by the thermodynamics of the reaction in the reactive complex ($\Delta G°'$) and work terms for bringing the reactants and products together in the proper orientation (W_R and W_P): $\Delta G^{\ddagger} = (\lambda/4)(1 + \Delta G°'/\lambda)^2 + W_R$, and $\Delta G°' = \Delta G° + W_P - W_R$. Often, λ is significantly larger than $\Delta G°'$, and the square term can be neglected, giving $\Delta G^{\ddagger} = \lambda/4 + \Delta G°'/2 + W_R$. Thus, for the comparison of the mutant and WT, $\Delta\Delta G^{\ddagger} \approx \Delta\lambda/4 + \Delta\Delta G°/2 + 1/2(\Delta W_P + \Delta W_R)$. Our redox potential measurements indicate that $\Delta\Delta G°$ is 1.8 kcal mol^{-1} for the mutant enzyme. Thus, the decrease in thermodynamic driving force is insufficient to account for the 3.2 kcal mol^{-1} change in $\Delta G^{\ddagger}$. Presumably, the transition state for the transfer of a hydride from NADPH to FAD is sensitive to the relative orientations of the reactants (Blankenhorn, 1975). Flavin-pyridine nucleotide charge–transfer complexes are often thought to be indicators of the proper orientation for rapid hydride transfer and have been observed as intermediates for PHBH in cases of fast reduction. When slow reduction occurs, the charge–transfer complexes are not observed (Entsch *et al.*, 1991b). The lack of observable charge–transfer complexes in the reduction reaction indicates that the orientation of the flavin and pyridine nucleotide is different in the mutant enzyme. If the same geometry for hydride transfer is operative in both Asn300Asp and WT, then the increase in $\Delta G^{\ddagger}$ would be the result of an increase in W_R and W_P, indicating an energy barrier to the proper orientation between the isoalloxazine and pyridine moieties. Alternatively, if no re-organization occurs, then a new transition-state geometry characterized by a higher intrinsic barrier is indicated. It is possible that the actual case lies between these extremes. It may be significant that the mutation is at the end of the loop of protein (residues 293–300) that forms a protein cage on the *re* side of the FAD where NADPH is known to bind (Manstein *et al.*, 1986).

Oxidative Half-Reaction. Changes in the substrate reactivity and changes in the flavin reactivity can explain the unusually slow oxidative half-reaction caused by the Asn300Asp mutation. The activation of the substrate by interactions with the enzyme is potentially complicated. Results from the Tyr201Phe mutant have highlighted the importance of the protonation state of the substrate for its reactivity toward hydroxylation. In the course of hydroxylation, the substrate hydroxyl must be deprotonated (Scheme 3, step 1) and reprotonated when the initial hydroxylation product re-aromatizes to form 3,4-diOHB (step 2). The effect of the

Scheme 3

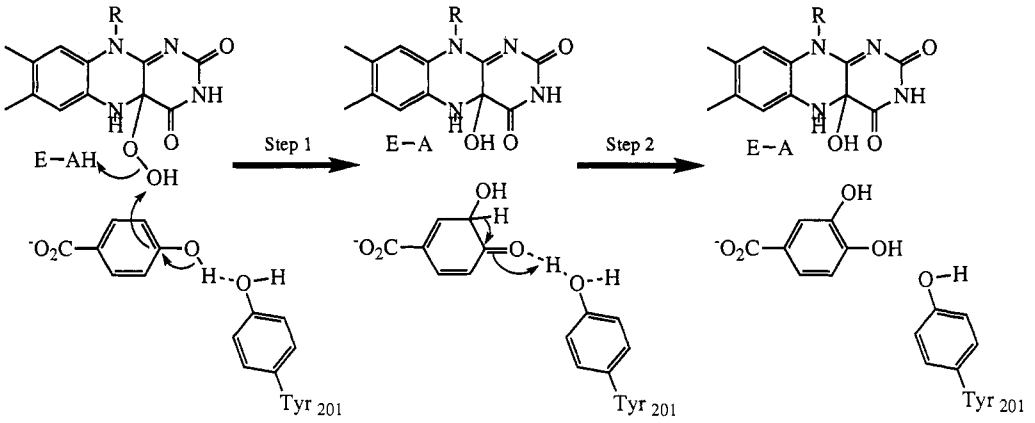

protein on the pK_a of *p*-OHB bound to EFlHOOH is probably similar to that observed with E_{OX}. We have shown that WT enzyme lowers the pK_a of bound *p*-OHB by 2 units. In contrast, the Tyr201Phe mutant does not lower the pK_a and, as a consequence, only hydroxylates to a small extent at a rate 10^3-fold slower than WT enzyme (Entsch *et al.*, 1991b). The importance of substrate reactivity has recently been reaffirmed by frontier orbital calculations (Vervoort *et al.*, 1992), which are consistent with our experimental observation that the phenolate form of the substrate is more reactive than the phenol form. However, the Asn300Asp mutant hydroxylates *p*-OHB completely (although 50-fold slower than WT enzyme), despite the lack of any observable *p*-OHB ionization. Thus, the importance of the protonation state of *p*-OHB must be more complex than originally postulated.

If the flavin hydroperoxide were only able to react with the phenolate form of the substrate, then at a pH below the pK_a of the enzyme-bound substrate a significant proportion of the hydroperoxide might be expected to eliminate H_2O_2 rather than react with *p*-OHB. However, this is not the case with the WT enzyme. A pK_a of 7.4 has been measured for *p*-OHB bound to oxidized WT enzyme, yet it hydroxylates *p*-OHB with 100% efficiency at pH 6.5. It should be noted that the rate of substrate exchange from the EFlHOOH is much lower than the rate of the hydroxylation reaction (Entsch *et al.*, 1976); thus, it is not possible to exchange the unreactive phenolic form of the substrate with the small proportion of phenolate that exists in solution at low pH. Some means for substrate activation and proton removal from the bound, solvent-inaccessible substrate seems necessary.

A hydrogen bond network extends from *p*-OHB to Tyr 201 to Tyr 385. While none of these residues is in direct contact with the solvent, the Tyr 385 side chain is 4–5 Å from a bound water molecule in the structure, which in turn is close to His 72, a residue accessible to bulk solvent. Thus, it seems possible that this tyrosine network could function as part of a proton relay system, shuttling a proton from *p*-OHB in order to activate it. Consistent with this hypothesis, we have recently obtained evidence by solvent isotope effect studies for the movement of more than one proton during the oxidation reactions (Palfey *et al.*, 1994). The decrease by 2 units in the phenolic pK_a of *p*-OHB bound to WT enzyme indicates that this H-O bond is significantly weaker than in solution. Thus, the H-O bond of the substrate is polarized significantly by the enzyme, requiring little change to achieve the transition state. The ability to polarize and exchange the phenolic proton via the tyrosine network has been removed in Tyr201Phe. The pathway for proton exchange remains intact in the Asn300Asp mutant, but the *p*-OHB H-O bond is less polarized than in WT enzyme. This is reflected in the lack of an observable shift in the pK_a of *p*-OHB in the mutant. The distance between the oxygen of *p*-OHB and Tyr201 in the WT·*p*-OHB complex crystal structure is 2.67 Å (Schreuder *et al.*, 1989). This distance has increased to 2.88 Å in the mutant enzyme, indicating a weakening of the *p*-OHB–Tyr201 hydrogen bond (Lah *et al.*, 1994). The polarization of the phenolic H-O bond might also explain how two similar enzymes, melilotate hydroxylase and phenol hydroxylase, are capable of activating their substrates, even though the phenolate was not observed in the enzyme–substrate complexes (Schopfer & Massey, 1980; Detmer & Massey, 1985).

Thus, the 50-fold decrease in hydroxylation rate seen in the Asn300Asp mutant can partly be explained by the less polarized, less acidic enzyme-bound *p*-OHB. This perturbation could be the result of the electrostatic repulsion between Asp 300 and the polarized or phenolate form of the substrate. The crystal structure of the Asn300Asp·*p*-OHB complex shows that the distance between these charges would be about 12 Å (Lah *et al.*, 1994). Other studies have shown that charge–charge interactions at this range often result in pK_a changes of around 0.5 unit (Gilson & Honig, 1987, 1988). Calculations of the electrostatic interactions are in qualitative agreement with an increase of the pK_a of 0.5–1 unit. Thus, charge–charge interactions do not completely explain this effect on *p*-OHB, and other changes observed in the mutant structure (Lah *et al.*, 1994) are also important. The fact that *p*-OHC ionizes on the enzyme with only a slightly higher pK_a than when bound to WT enzyme indicates that this ligand is not binding identically to *p*-OHB. This is consistent with the inability of the WT enzyme to hydroxylate *p*-OHC.

While the change in the strength of the hydrogen bond between *p*-OHB and Tyr 201 undoubtedly affects substrate reactivity in Asn300Asp, it is insufficient to explain completely the changes in the hydroxylation reaction, and it does not address the 150-fold slowing of the conversion of EFlHOH to oxidized enzyme in the Asn300Asp mutant. Changes in the flavin reactivity must be considered as well. The elimination of H_2O_2 from WT enzyme in the presence of *p*-OHB is modeled by the Tyr201Phe mutant (Entsch *et al.*, 1991b). A rate constant of 0.72 s^{-1} was found for this elimination reaction. In WT enzyme, the oxygen-transfer reaction (47 s^{-1}) competes effectively with this reaction, leading to no detectable H_2O_2 production. However, the oxygen-transfer rate for the Asn300Asp mutant is only 1.1 s^{-1}, which is very similar to the rate for elimination of H_2O_2 from Tyr201Phe. If the EFlHOOH of Asn300Asp were also to eliminate H_2O_2 at 0.7 s^{-1}, only about 60% hydroxylation would occur instead of the observed 100% substrate hydroxylation.

Therefore, the mutation has also decreased the rate of elimination of H_2O_2 from EFlHOOH. The elimination of water from EFlHOH to form the oxidized flavin is also significantly slower than in WT enzyme. Since the mechanism of H_2O_2 elimination from EFlHOOH should be analogous to the elimination of H_2O from EFlHOH, it is reasonable to expect both elimination reactions to be affected similarly by the mutation.

Several origins for altered Asn300Asp flavin reactivity are possible. The introduction of a negative charge near the flavin could cause electronic perturbations by electrostatic forces. The various spectral changes and the changes in E_{m7} are direct indications of electronic perturbations. The crystal structure of the mutant enzyme shows a slight shift in the axis of helix H10, changing the region where it exerts its inductive effect (Lah *et al.*, 1994). Furthermore, the close contact of the flavin O(2) with the amide nitrogen of Asn 300 is absent in the mutant enzyme and replaced by a weaker hydrogen bond to a water molecule (0.5–0.6 Å longer). One or a combination of several of these structural effects may be responsible for the observed decrease in the elimination rates for the C(4a)-flavin adducts. A necessary event in these elimination reactions is the deprotonation of N(5) of the flavin. The electronic changes in the mutant may increase the electron density at N(5), increasing the pK_a in the transition state, thus slowing the reaction. Another possible consequence of electronic perturbations to the flavin is a decrease in the electrophilicity of the hydroperoxide. It is unclear, then, to what degree the lower reactivity of the flavin hydroperoxide and the lower reactivity of *p*-OHB are responsible for the low oxygen-transfer rate with Asn300Asp.

Interestingly, with *p*-OHB bound to the enzyme, the reduced flavin of the Asn300Asp mutant enzyme is as reactive or possibly more reactive with O_2 than is WT enzyme. Free reduced flavin reacts much more slowly with oxygen than enzyme-bound flavin (Massey *et al.*, 1971; Kemal & Bruice, 1976). The enzyme is a necessary promoter of this reaction, exerting its effects by unknown means. The introduction of a negative charge near the FAD by mutation has not decreased this reactivity and seems to have increased it slightly. This is consistent with the mechanism proposed by Bruice for EFlHOOH formation (Bruice, 1984), involving a rate-determining electron transfer from $FADH^-$ to O_2, to form an intermediate radical pair, which quickly collapses to the hydroperoxide. The 40 mV decrease in the potential of the Asn300Asp·*p*-OHB complex would make the initial electron transfer to O_2 more favorable.

In the absence of substrate, the mutant and WT enzymes both react with oxygen at similar rates, and neither forms an observable EFlHOOH. In the presence of 0.1 M azide, similar proportions of both enzymes react to form EFlHOOH, which decays to oxidized enzyme at the same rate for both Asn300Asp and WT enzyme. Thus, without *p*-OHB at the active site, the mutant and WT enzyme-bound reduced flavins have the same reactivities. The stabilizing effect of the Asn300Asp mutation on C(4a) adducts depends on the presence of substrate. The structural basis for this is unclear, since the structures of the ligand-free enzymes are not known to high resolution.

Azide Effects. Our experiments have provided additional insight into the origin of the inhibitory effects of monovalent anions. Azide binds to the *p*-OHB site (or a site competitive with *p*-OHB), but this is not the site that provides the stabilization of intermediates since substrate binding to its site is slow. Instead, the inhibitory site appears to be rapidly accessible to solvent, probably at the surface. The small effects of azide on the mutant can be understood in light of results obtained for PHBH from *P. desmolytica* (Shoun *et al.*, 1983). It was observed that monovalent anions prevent the ionization of enzyme-bound *p*-OHB. Since the mutation has achieved this effect already, there is little additional effect to be gained by binding anions. A detailed understanding of the monovalent anion effects awaits further chemical and structural study.

Conclusion. The mutation of Asn 300 to Asp has resulted in catalytic, dynamic, and structural changes to PHBH. Several interactions (electrostatic as well as hydrogen bonding) are provided by the protein in order to lower the substrate pK_a, and no single residue is solely responsible for these influences. Conversely, our results with this and other PHBH mutants illustrate a general caveat for interpreting site-directed mutagenesis studies—a single active-site residue will have a role in many or all of the processes comprising the catalytic cycle. In the case of PHBH, we are fortunate because we can directly observe many of these individual effects.

ACKNOWLEDGMENT

The authors thank Mr. Ronald E. Wicks (University of New England) for his skilled help in the production of the mutant enzyme described in this paper and Dr. Martha L. Ludwig (University of Michigan) for helpful discussions of this paper.

REFERENCES

Ballou, D. P. (1984) in *Flavins and Flavoproteins* (Bray, R. C., Engel, P. C., & Mayhew, S. G., Eds.) pp 605–618, Walter de Gruyter, Berlin.

Barshop, B. A., Wreen, R. F., & Frieden, C. (1983) *Anal. Biochem. 130*, 134–145.

Blankenhorn, G. (1984) *Eur. J. Biochem. 50*, 351–356.

Bruice, T. C. (1984) in *Flavins and Flavoproteins* (Bray, R. C., Engel, P. C. & Mayhew, S. G., Eds.) pp 45–55, Walter de Gruyter, Berlin.

Detmer, K., & Massey, V. (1985) *J. Biol. Chem. 260*, 5998–6005.

Entsch, B. (1990) *Methods Enzymol. 188*, 138–147.

Entsch, B., & Ballou, D. P. (1989) *Biochim. Biophys. Acta 999*, 313–322.

Entsch, B., Ballou, D. P., & Massey, V. (1976) *J. Biol. Chem. 251*, 2550–2563.

Entsch, B., Nan, Y., Weaich, K., & Scott, K. F. (1988) *Gene 71*, 279–291.

Entsch, B., Palfey, B. A., Ballou, D. P., & Massey, V. (1991a) in *Flavins and Flavoproteins* (Ronchi, S., Curti, B., & Zanetti, G., Eds.) pp 219–230, Walter de Gruyter, Berlin.

Entsch, B., Palfey, B. A., Ballou, D. P., & Massey, V. (1991b) *J. Biol. Chem. 266*, 17341–17349.

Gibson, Q. H., Swoboda, B. E. P., & Massey, (1964) *J. Biol. Chem. 239*, 3927–3934.

Gilson, N. K., & Honig, B. H. (1987) *Nature 330*, 84–88.

Gilson, N. K., & Honig, B. H. (1988) *Proteins 3*, 32–52.

Howell, L. G., Spector, T., & Massey, V. (1972) *J. Biol. Chem. 247*, 4340–4350.

Husain, M., & Massey, V. (1979) *J. Biol. Chem. 254*, 6657–6666.

Kemal, C., & Bruice, T. C. (1976) *Proc. Natl. Acad. Sci. U.S.A. 73*, 995–999.

Kunkel, T. A.; Roberts, J. D., & Zakour, R. A. (1987) *Methods Enzymol. 154*, 367–382.

Lah, M. S., Palfey, B. A., Schreuder, H. A., & Ludwig, M. L. (1994) *Biochemistry* (following paper in this issue).

Lowry, T. H., & Richardson, K. S. (1987) *Mechanism and Theory in Organic Chemistry*, 3rd ed., pp 222–227, Harper & Row, Publishers, Inc., New York.
Manstein, D. J., Pai, E. F., Schopfer, L. M., & Massey, V. (1986) *Biochemistry 25*, 6807–6816.
Massey, V. (1991) in *Flavins and Flavoproteins* (Ronchi, S., Curti, B., & Zanetti, G., Eds.) pp 59–66, Walter de Gruyter, Berlin.
Massey, V., & Palmer, G. (1966) *Biochemistry 5*, 3181–3189.
Massey, V., Palmer, G., & Ballou, D. P. (1971) in *Flavins and Flavoproteins* (Kamin, H., Ed.) pp 349–361, University Park Press, Baltimore, MD.
Müller, F., Voordouw, G., van Berkel, W. J. H., Steennis, P. J., Visser, S., & van Rooijen, P. J. (1979) *Eur. J. Biochem. 101*, 235–244.
Palfey, B. A., Ballou, D. P., & Massey, V. (1994) in *Flavins and Flavoproteins*, Walter de Gruyter, Berlin (in press).
Schopfer, L. M., & Massey, V. (1980) *J. Biol. Chem. 255*, 5355–5363.
Schopfer, L. M., Wessiak, A., & Massey, V. (1991) *J. Biol. Chem. 266*, 13080–13085.
Schreuder, H. A., van der Laan, J. M., Hol, W. G. J., & Drenth, J. (1988) *J. Mol. Biol. 199*, 637–648.
Schreuder, H. A., Prick, P. A. J., Wieringa, R. K., Vriend, G., Wilson, K. S., Hol, W. G. J., & Drenth, J. (1989) *J. Mol. Biol. 208*, 679–696.
Schreuder, H. A., Hol, W. G. J., & Drenth, J. (1990) *Biochemistry 29*, 3101–3108.
Schreuder, H. A., van der Laan, J. M., Swarte, M. B. A., Kalk, K. A., Hol, W. G. J., & Drenth, J. (1992) *Proteins: Struct., Funct., Genet. 14*, 178–190.
Sejlitz, T., & Neujahr, H. Y. (1987) *Eur. J. Biochem. 170*, 343–349.
Shoun, H., Higashi, N., Beppu, T., Nakamura, S., Hiromi, K., & Arima, K. (1979) *J. Biol. Chem. 254*, 10944–10951.
Shoun, H., Arima, K., & Beppu, T. (1983) *J. Biochem. 93*, 169–176.
Steennis, P. J., Cordes, M. M., Hilkens, J. G. H., & Müller, F. (1973) *FEBS Lett. 36*, 177–180.
Strickland, S., Palmer, G., & Massey, V. (1975) *J. Biol. Chem. 259*, 4048–4052.
Sühnel, J., & Schowen, R. L. (1991) in *Enzyme Mechanism from Isotope Effects* (Cook, P. F., Ed.) pp 3–35, CRC Press, Inc., Boca Raton.
van Berkel, W. J. H., & Müller, F. (1987) *Eur. J. Biochem. 167*, 35–46.
van der Laan, J. M. (1986) Doctoral Dissertation, University of Groningen, The Netherlands.
van der Laan, J. M., Schreuder, H. A., Swarte, M. B. A., Wierenga, R. K., Kalk, K. H., & Hol, W. G. J. (1989) *Biochemistry 28*, 7199–7205.
Vervoort, J., Rietjens, M. C. M., van Berkel, J. H., & Veeger, C. (1992) *Eur. J. Biochem. 206*, 479–484.
Wessiak, A., Schopfer, L. M., & Massey, V. (1984) *J. Biol. Chem. 259*, 12547–12556.